

Pramote Dechaumphai  
Associate Professor

Jittin Triputtarat  
Supatpong Sikkhabandit  
Graduate Students

Mechanical Engineering Department  
Chulalongkorn University  
Bangkok, Thailand

# A Finite Element Method for Viscous Incompressible Flow Analysis

*A finite element method for viscous incompressible flow analysis is presented. The flow is classified into two types namely: the flow without inertia for slow moving fluid, and with inertia for a more general flow. Finite element equations corresponding to these flows are derived and are used in the development of the computer programs that can be executed on standard personal computers. The programs have been verified by solving academic-type examples that have exact solutions before applying to solve more complex flow problems.*

## 1. Introduction

The finite element method is one of the numerical methods that has received the popularity due to its capability for solving complex structural problems [1,2]. The method has been extended to solve problems in several other fields such as in the field of heat transfer [3, 4], electromagnetics [5], biomechanics [6], etc. In spite of the great success of the method in these fields, its application to fluid mechanics, particularly to viscous flows, is still under intensive research. This is due to the fact that the governing differential equations for general flow problems consist of several coupled equations which are inherently nonlinear. Accurate numerical solutions thus require vast amount of computer time and data storage. One way to minimize the amount of computer time and data storage used is to employ an adaptive meshing technique [7,8]. The technique places small elements in the regions of large change in the solution gradients to increase solution accuracy, and at the same time, uses large elements in the other regions to reduce the computational time and computer memory.

As the first step toward accurate flow solutions using adaptive meshing technique, this paper investigates and develops a finite element formulation suitable for analyses of general incompressible flow problems. The selected formulation is evaluated in this paper and will be used together with the adaptive meshing technique in the future. The paper starts with viscous incompressible flow without inertia for slow moving fluid. The corresponding Navier-Stokes equations are used to derive the finite element equations. The computational procedure used in the development of the computer program is described. The same process is repeated but for viscous incompressible flow with inertia for general flow. Several examples and applications are then presented to evaluate and demonstrate the capability of the finite element formulation for analysis of viscous incompressible flows.

## 2. Viscous Incompressible Flow Without Inertia

### 2.1 Governing Equations

The fundamental laws used to solve for fluid motion in a general form are the law of: (a) conservation

of mass or continuity equation, (b) conservation of momentums, and (c) conservation of energy, which constitute a set of coupled, nonlinear, partial differential equations. For low-speed incompressible flow, the fluid density and the flow temperature are assumed constant, and only the continuity equation and the momentum equations are needed for the analysis. These differential equations for the two-dimensional steady-state flow are,

$$\frac{\partial u}{\partial x} + \frac{\partial v}{\partial y} = 0 \quad (1a)$$

$$\mu \left( \frac{\partial^2 u}{\partial x^2} + \frac{\partial^2 u}{\partial y^2} \right) - \frac{\partial p}{\partial x} = \rho \left( u \frac{\partial u}{\partial x} + v \frac{\partial u}{\partial y} \right) \quad (1b)$$

$$\mu \left( \frac{\partial^2 v}{\partial x^2} + \frac{\partial^2 v}{\partial y^2} \right) - \frac{\partial p}{\partial y} = \rho \left( u \frac{\partial v}{\partial x} + v \frac{\partial v}{\partial y} \right) \quad (1c)$$

where  $u$  and  $v$  are the velocity components in the  $x$  and  $y$  direction, respectively;  $p$  is the pressure,  $\mu$  is the fluid viscosity coefficient and  $\rho$  is the fluid density.

The case of viscous incompressible flow without inertia can be categorized by low Reynolds number, which represents the ratio of inertial forces to viscous forces in a fluid motion. When the Reynolds number is very small, the inertial forces are insignificant compared to the viscous forces and can be omitted from the governing momentum equations, Eqs. (1b-c). Small Reynolds numbers characterize slow moving flows and flows of very viscous fluids. In this case, the set of differential equations (Eqs. (1a-c)) for constant fluid properties reduces to a simpler form and can be rewritten using tensor notations as,

$$u_{,x} + v_{,y} = 0 \quad (2a)$$

$$\sigma_{x,x} + \tau_{xy,y} = 0 \quad (2b)$$

$$\tau_{xy,x} + \sigma_{y,y} = 0 \quad (2c)$$

where the stress components are,

$$\sigma_x = -p + 2\mu u_{,x} \quad (3a)$$

$$\sigma_y = -p + 2\mu v_{,y} \quad (3b)$$

$$\tau_{xy} = \mu(u_{,y} + v_{,x}) \quad (3c)$$

The differential equations, Eqs. (2a-c), are to be solved together with appropriate boundary conditions of either specifying velocity components along edge  $S_1$ ,

$$u = u_1(x, y) \quad (4a)$$

$$v = v_1(x, y) \quad (4b)$$

or surface tractions along edge  $S_2$ ,

$$T_x = \sigma_x \ell + \tau_{xy} m \quad (5a)$$

$$T_y = \tau_{xy} \ell + \sigma_y m \quad (5b)$$

where  $\ell$  and  $m$  are the direction cosines of the unit vector normal to the boundary edge.

## 2.2 Finite Element Formulation

The basic unknowns for the two-dimensional viscous incompressible flow problem corresponding to the continuity Eq. (1a) and the two momentum Eqs. (1b-c) are the velocity components  $u$ ,  $v$  and the pressure  $p$ . The six-node triangular element suggested in Ref. [9] is used in this study. The element assumes quadratic interpolation for the velocity component distributions and linear interpolation for the pressure distribution in the following forms,

$$u(x, y) = N_\alpha u_\alpha \quad (6a)$$

$$v(x, y) = N_\alpha v_\alpha \quad (6b)$$

$$p(x, y) = H_\lambda p_\lambda \quad (6c)$$

where  $\alpha = 1, 2, \dots, 6$ ;  $\lambda = 1, 2, 3$ ;  $N_\alpha$  and  $H_\lambda$  are the element interpolation functions for the velocity and pressure, respectively.

To derive the finite element equations, the method of weighted residuals [4] is applied to the momentum Eqs. (2b-c) and the continuity Eq. (2a),

$$\int_A N_i (\sigma_{x,x} + \tau_{xy,y}) dA = 0 \quad (7a)$$

$$\int_A N_i (\tau_{xy,x} + \sigma_{y,y}) dA = 0 \quad (7b)$$

$$\int_A H_i (u_{,x} + v_{,y}) dA = 0 \quad (7c)$$

where  $A$  is the element area. Gauss's theorem is then applied to Eqs. (7a-b) to generate the boundary integral terms associated with the surface tractions. With the use of Eqs. (5a-b), Eqs. (7a-b) become,

$$\begin{aligned} \int_A \left[ (2\mu u_{,x} - p) N_{\alpha,x} + \mu (u_{,y} + v_{,x}) N_{\alpha,y} \right] dA \\ = \int_{S_2} N_\alpha T_x dS \end{aligned} \quad (8a)$$

$$\begin{aligned} \int_A \left[ \mu (u_{,y} + v_{,x}) N_{\alpha,x} + (2\mu u_{,y} - p) N_{\alpha,y} \right] dA \\ = \int_{S_2} N_\alpha T_y dS \end{aligned} \quad (8b)$$

Applying the element velocity component distributions and the pressure distribution, Eqs. (6a-c), the finite element equations can be written in the form,

$$\begin{aligned} (2\mu M_{\alpha\beta xx} + \mu M_{\alpha\beta yy}) u_\beta + \mu M_{\alpha\beta xy} v_\beta - H_{\alpha\lambda x} p_\lambda \\ = R_{\alpha x} \end{aligned} \quad (9a)$$

$$\begin{aligned} \mu M_{\alpha\beta yx} u_\beta + (\mu M_{\alpha\beta xx} + 2\mu M_{\alpha\beta yy}) v_\beta - H_{\alpha\lambda y} p_\lambda \\ = R_{\alpha y} \end{aligned} \quad (9b)$$

$$H_{\beta\lambda x} u_\beta + H_{\beta\lambda y} v_\beta = 0 \quad (9c)$$

where

$$M_{\alpha\beta xx} = \int_A N_{\alpha,x} N_{\beta,x} dA \quad (10a)$$

$$M_{\alpha\beta yy} = \int_A N_{\alpha,y} N_{\beta,y} dA \quad (10b)$$

$$M_{\alpha\beta xy} = \int_A N_{\alpha,x} N_{\beta,y} dA \quad (10c)$$

$$M_{\alpha\beta yx} = \int_A N_{\alpha,y} N_{\beta,x} dA \quad (10d)$$

$$H_{\alpha\lambda x} = \int_A N_{\alpha,x} H_\lambda dA \quad (10e)$$

$$H_{\alpha\lambda y} = \int_A N_{\alpha,y} H_\lambda dA \quad (10f)$$

$$R_{\alpha x} = \int_{S_2} N_\alpha T_x dS \quad (10g)$$

$$R_{\alpha y} = \int_{S_2} N_\alpha T_y dS \quad (10h)$$

These element matrices can be evaluated in closed form ready for computer programming. Details of the derivation for these element matrices are omitted herein for brevity.

## 2.3 Computational Procedure

The closed form finite element matrices, Eqs. (10a-h), for the six-node triangular element are used in the development of a computer program. The program is written in FORTRAN and can be executed on standard personal computers. For each element, the element equations (9a-c) which consist of 15 equations are established. These element equations are then assembled to form up a system of equations for the problem considered. Appropriate boundary conditions are then applied before solving for the unknowns of the nodal velocity components and pressures. It should be noted that the element equations (9a-c) are linear, thus the system of equations can be solved directly. Both the finite element matrices derived and the computer program developed have been verified by a number of simple examples that have exact solutions such as the one described in the next section prior to applying to solve more complex problems.

## 2.4 Example

To evaluate the finite element computer program developed, the fully-developed flow between parallel plates (Poiseuille flow) as shown in Fig. 1 is used. The inlet velocity profile is in the form of parabolic distribution given by,

$$u(y) = \frac{4y}{h^2} (h-y) \quad (11)$$

The exact velocity profile at any  $x$ -location can be derived [10] and written in the form,

$$u(y) = \frac{y}{2\mu} (y-h) \frac{\partial p}{\partial x} \quad (12)$$

The finite element model with 12 triangles and 35 nodes and the boundary conditions are shown in Fig. 2. With this model, the computer program was used to solve for flow field velocity and pressure distributions. Figure 3 shows the predicted flow velocity profiles which are identical along the x-direction of the flow. These predicted velocity profiles are identical to the exact solution, Eq. (12), as compared in Fig. 4. Figure 5 shows the predicted pressure distributions on the lower and upper plates and on the center line along the flow direction. These predicted pressure distributions agree with the exact solution,

$$p(x) = -\frac{8\mu}{h^2} (x-30) \quad (13)$$

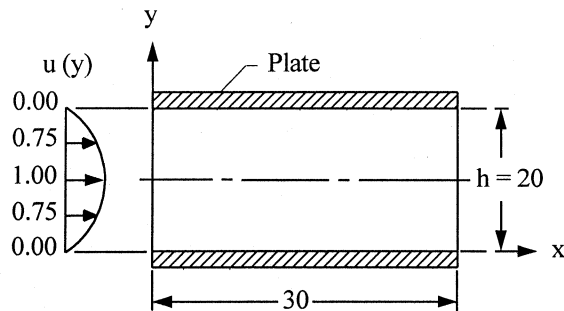


Fig. 1 - Flow between parallel plates.

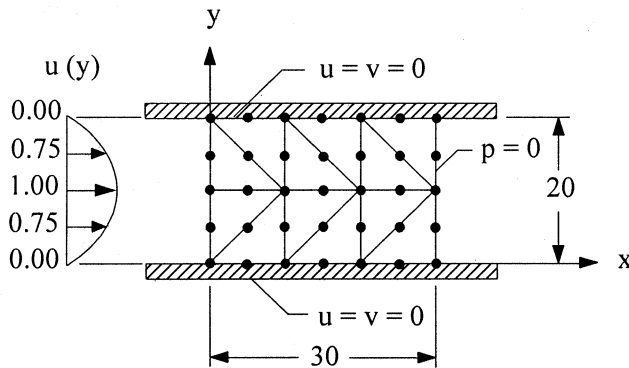


Fig. 2 - Finite element model and boundary conditions for flow between parallel plates.

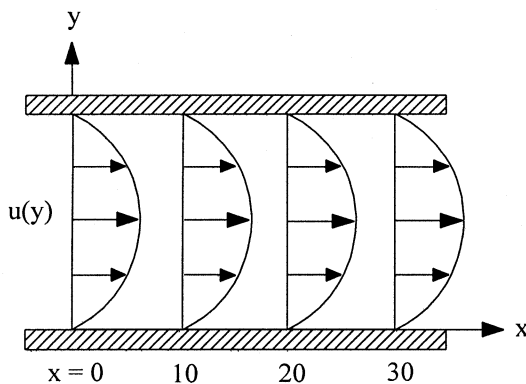


Fig. 3 - Predicted flow velocity profiles along x-direction of flow between parallel plates.

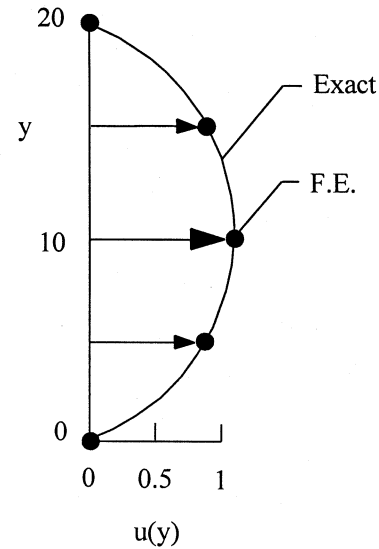


Fig. 4 - Comparative flow velocity profiles between exact and finite element solutions.

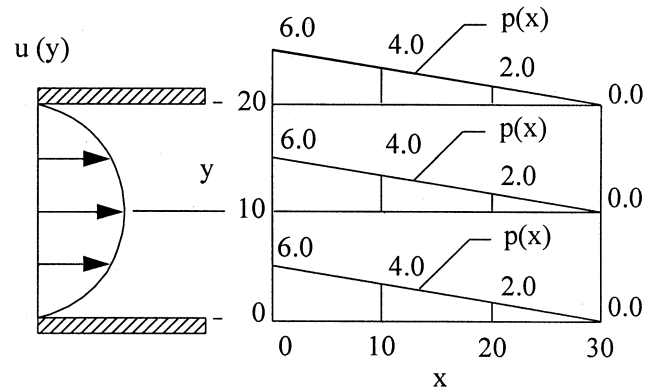


Fig. 5 - Predicted pressure distributions along x-direction.

### 3. Viscous Incompressible Flow With Inertia

#### 3.1 Governing Equations

For more general flow problems, the Navier-Stokes equations, Eqs. (1a-c), must be solved. These equations are inherently nonlinear because of the presence of the inertia terms shown on the right-hand-side of Eqs. (1b-c). These Navier-Stokes equations are rewritten using tensor notations for clarity in the derivation of finite element equations in the next section,

$$u_{,x} + v_{,y} = 0 \quad (14a)$$

$$u u_{,x} + v u_{,y} - \sigma_{x,x} - \tau_{xy,y} = 0 \quad (14b)$$

$$u v_{,x} + v v_{,y} - \tau_{xy,x} - \sigma_{y,y} = 0 \quad (14c)$$

where the stress components are now defined by,

$$\sigma_x = -p/\rho + 2\nu u_{,x} \quad (15a)$$

$$\sigma_y = -p/\rho + 2\nu v_{,y} \quad (15b)$$

$$\tau_{xy} = \nu (u_{,y} + v_{,x}) \quad (15c)$$

and the kinematics viscosity,

$$\nu = \frac{\mu}{\rho} \quad (16)$$

The above set of coupled nonlinear partial differential equations, Eqs. (14a-c), are to be solved together with the boundary conditions of specified velocity components (Eqs. (4a-b)) or surface tractions (Eqs. (5a-b)) along edges.

### 3.2 Finite Element Formulation

The method of weighted residuals [4] is applied to the differential equations, Eqs. (14a-c), to derive the finite element equations in the same fashion as for the case of flow without inertia. The same six-node triangular element with the velocity component and pressure distributions given by Eqs. (6a-c) is used. The procedure leads to the finite element equations in the nonlinear form as,

$$K_{\alpha\beta\gamma x} u_\beta u_\gamma + K_{\alpha\beta\gamma y} v_\beta u_\gamma - H_{\alpha\lambda x} p_\lambda + S_{\alpha\beta xx} u_\beta + S_{\alpha\beta xy} v_\beta = Q_{\alpha x} \quad (17a)$$

$$K_{\alpha\beta\gamma x} u_\beta v_\gamma + K_{\alpha\beta\gamma y} v_\beta v_\gamma - H_{\alpha\lambda y} p_\lambda + S_{\alpha\beta yx} u_\beta + S_{\alpha\beta yy} v_\beta = Q_{\alpha y} \quad (17b)$$

$$H_{\beta\mu x} u_\beta + H_{\beta\mu y} v_\beta = 0 \quad (17c)$$

where the coefficients in element matrices are in form of the integrals over the element area  $A$  and along the edge  $S_2$  as,

$$K_{\alpha\beta\gamma x} = \int_A N_\alpha N_\beta N_{\gamma,x} dA \quad (18a)$$

$$K_{\alpha\beta\gamma y} = \int_A N_\alpha N_\beta N_{\gamma,y} dA \quad (18b)$$

$$H_{\alpha\lambda x} = \int_A N_{\alpha,x} H_\lambda dA \quad (18c)$$

$$H_{\alpha\lambda y} = \int_A N_{\alpha,y} H_\lambda dA \quad (18d)$$

$$S_{\alpha\beta xx} = \int_A 2 v N_{\alpha,x} N_{\beta,x} dA + \int_A v N_{\alpha,y} N_{\beta,y} dA \quad (18e)$$

$$S_{\alpha\beta xy} = \int_A v N_{\alpha,y} N_{\beta,x} dA \quad (18f)$$

$$S_{\alpha\beta yx} = \int_A v N_{\alpha,x} N_{\beta,y} dA \quad (18g)$$

$$S_{\alpha\beta yy} = \int_A v N_{\alpha,x} N_{\beta,x} dA + \int_A 2 v N_{\alpha,y} N_{\beta,y} dA \quad (18h)$$

$$Q_{\alpha x} = \int_{S_2} N_i T_x dS \quad (18i)$$

$$Q_{\alpha y} = \int_{S_2} N_i T_y dS \quad (18j)$$

These element matrices can be evaluated in closed form and detailed derivation is omitted herein for brevity.

### 3.3 Computational Procedure

The derived finite element equations, Eqs. (17a-c), are nonlinear. These nonlinear algebraic equations are solved using the Newton-Raphson iteration technique [11] by first writing the unbalanced values from a given set of solutions for the finite element Eqs. (17a-c) as,

$$F_{\alpha x} = K_{\alpha\beta\gamma x} u_\beta u_\gamma + K_{\alpha\beta\gamma y} v_\beta u_\gamma - H_{\alpha\lambda x} p_\lambda + S_{\alpha\beta xx} u_\beta + S_{\alpha\beta xy} v_\beta - Q_{\alpha x} \quad (19a)$$

$$F_{\alpha y} = K_{\alpha\beta\gamma x} u_\beta v_\gamma + K_{\alpha\beta\gamma y} v_\beta v_\gamma - H_{\alpha\lambda y} p_\lambda + S_{\alpha\beta yx} u_\beta + S_{\alpha\beta yy} v_\beta - Q_{\alpha y} \quad (19b)$$

$$F_\mu = H_{\beta\mu x} u_\beta + H_{\beta\mu y} v_\beta \quad (19c)$$

The application of the Newton-Raphson iteration technique leads to a set of algebraic equations with the incremental unknowns in the form,

$$G_{\alpha\beta x} \Delta u_\beta + L_{\alpha\beta y} \Delta v_\beta - H_{\alpha\lambda x} \Delta p_\lambda = F_{\alpha x} \quad (20a)$$

$$L_{\alpha\beta x} \Delta u_\beta + G_{\alpha\beta y} \Delta v_\beta - H_{\alpha\lambda y} \Delta p_\lambda = F_{\alpha y} \quad (20b)$$

$$H_{\beta\mu x} \Delta u_\beta + H_{\beta\mu y} \Delta v_\beta = F_\mu \quad (20c)$$

where

$$G_{\alpha\beta x} = K_{\alpha\beta\gamma x} u_\gamma + K_{\alpha\gamma\beta x} u_\gamma + K_{\alpha\gamma\beta y} v_\gamma + S_{\alpha\beta xx} \quad (21a)$$

$$G_{\alpha\beta y} = K_{\alpha\beta\gamma y} v_\gamma + K_{\alpha\gamma\beta y} v_\gamma + K_{\alpha\gamma\beta x} u_\gamma + S_{\alpha\beta yy} \quad (21b)$$

$$L_{\alpha\beta x} = K_{\alpha\beta\gamma x} v_\gamma + S_{\alpha\beta xy} \quad (21c)$$

$$L_{\alpha\beta y} = K_{\alpha\beta\gamma y} u_\gamma + S_{\alpha\beta yx} \quad (21d)$$

In these Eqs. (21a-d),  $u_\gamma$  and  $v_\gamma$  are the values of the velocity components at the  $i^{\text{th}}$  iteration. The iteration process is terminated if the percentage of the overall error is less than the specified value.

The final form of the finite element equations, Eqs. (20-21), and the iteration procedure described are used in the development of the second finite element computer program. The program is also written in FORTRAN and can be executed on standard personal computers. The main objective in the development of this computer program is such that it follows the formulation derived, easy to understand, and will be used together with the adaptive meshing technique later. Both the formulation derive and the computer program developed have been verified by several examples that have exact solution and/or experimental results before applying to solve more complex flow problems. Selected example and an application are presented in the next section.

### 3.4 Example and Application

The first example selected for evaluating the finite element computer program for viscous incompressible flow with inertia is the Couette flow problem. The problem geometry and the boundary conditions are shown in Fig. 6. The top plate moves to the right with the velocity of  $u=1$  while the bottom plate moves to the left with the velocity of  $u=-0.5$ . The finite element model consisting of 18 elements and 49 nodes is also shown in the figure. The exact  $u$ -velocity distribution for the entire flow field can be derived [10] and is given by,

$$u(y) = 1.5y - 0.5 \quad (22)$$

The problem was analyzed by the computer program developed and the predicted flow velocity profiles which are identical at any x-location along the flow direction as shown in Fig. 7. These predicted velocity profiles are compared and found to be identical to the exact solution, Eq. (22), as shown in Fig. 8.

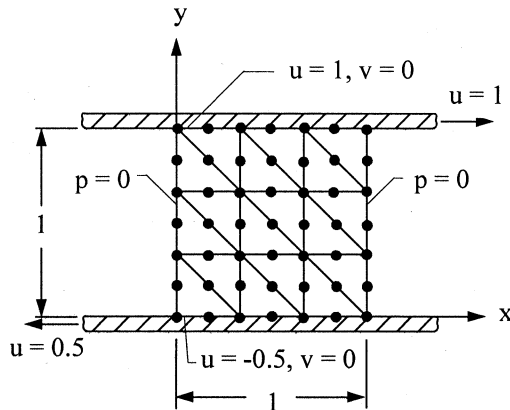


Fig. 6 - Finite element model and boundary conditions for Couette flow.

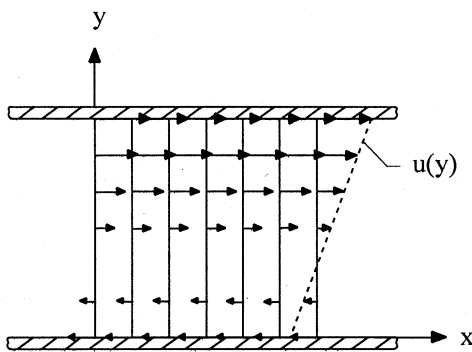


Fig. 7 - Predicted flow velocity profiles along x-direction for Couette flow.

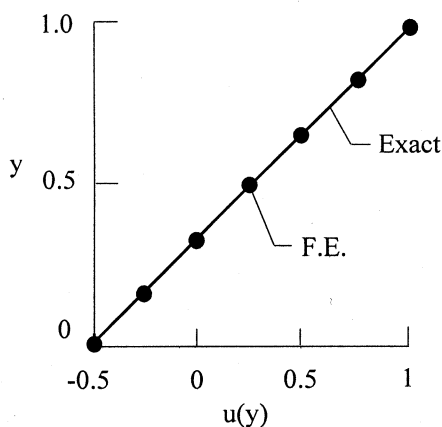


Fig. 8 - Comparative flow velocity profile between exact and finite element solutions.

The demonstrate the capability of the computer program for solving flow behavior of a more complex problem, a flow through a duct shown in Fig. 9 is simulated. The duct is in the main electricity generating plant of the Electricity Generating Authority located at the northern section of Bangkok, Thailand. As shown in the figure, the duct has uncommon shape with varying cross-sectional area. Flow circulation that causes erosion is suspected at the upper left corner of the duct. Figure 9 also shows the finite element model with 233 triangles and 516 nodes. The flow velocity profile at the top inlet of the duct is assumed in the form of parabola with the Reynolds number of 100.

With the problem statement and the finite element model shown in Fig. 9, the finite element computer program was used to predict the flow behavior. The result of the flow field is shown by the velocity vectors in Fig. 10. The velocity vectors indicate the area of flow circulation as previously suspected. Detail of the flow circulation behavior in this area is enlarged and shown in Fig. 11.

To avoid the flow circulations, two guided plates are placed at the top section of the duct to control the flow behavior as shown in Fig. 12. The figure also shows the finite element model that consists of 388 triangles and 869 nodes. The analysis was repeated and the predicted flow velocity vectors are shown in Fig. 13. The figure indicates the disappearance of the flow circulation. Figure 14 also highlights the detail of the flow behavior near the plate exits. The predicted flow solutions demonstrate the capability of the finite element formulation and the computer program developed that can help engineers to increase understanding of the flow behavior in order to correct the problem or to improve the design.

#### 4. Concluding Remarks

A finite element method for analysis of viscous incompressible flow problems is presented. The Navier-Stokes equations consisting of the conservation of mass and momentums are solved. The flow is classified into two types, i.e., the flow without inertia for slow moving fluid, and with inertia for a more general flow. For both types, the finite element equations were derived and the corresponding computer programs have been developed. These computer programs will be used together with the adaptive meshing technique in the future to improve the flow solution accuracy as well as to reduce the computational time and memory.

In the case of flow without inertia for slow moving fluid, the finite element equations are linear and direct solution technique can be used to solve for nodal unknowns. For a more general flow, the inertia terms are included in the Navier-Stokes equations resulting in nonlinear differential equations. The derived finite element equations are thus nonlinear requiring an iterative technique solver. The Newton-Raphson iteration method is applied to solve for the nodal unknowns.

Both the finite element formulations and the corresponding computer programs developed have been

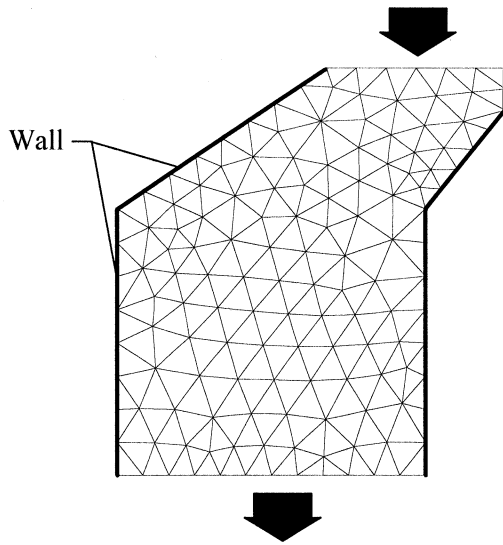


Fig. 9 - Finite element model with 233 triangles and 516 nodes for flow through a duct.

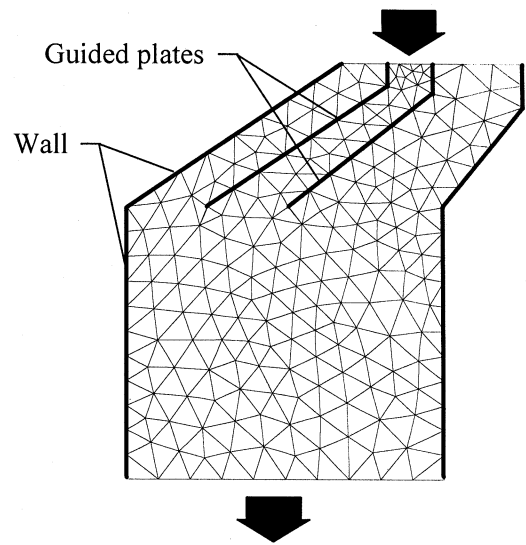


Fig. 12 - Finite element model using 388 triangles and 869 nodes for flow through duct with guided plates.

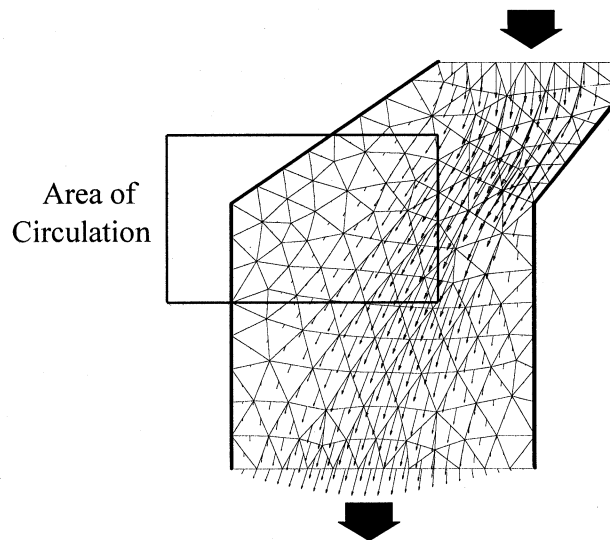


Fig. 10 - Predicted flow behavior by velocity vectors with area of circulation.

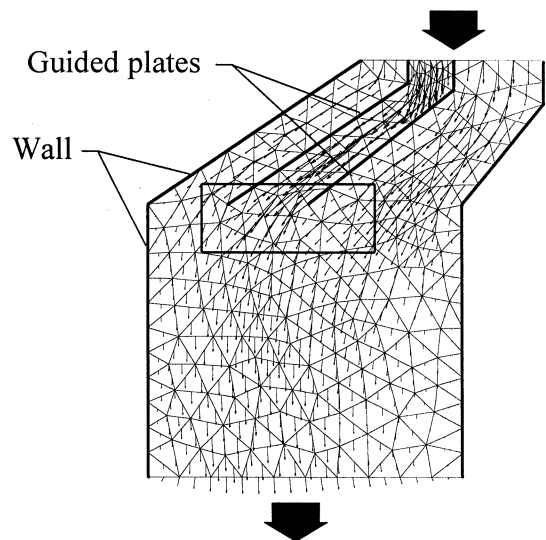


Fig. 13 - Predicted flow velocity vectors in duct with guided plates.

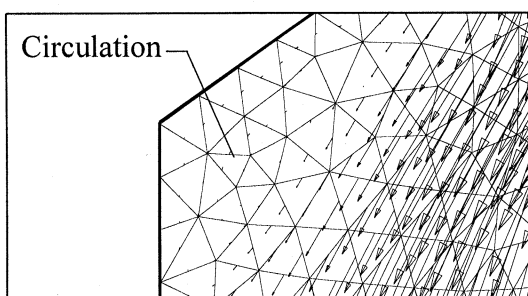


Fig. 11 - Detail of flow circulation in the area highlighted in Fig. 10.

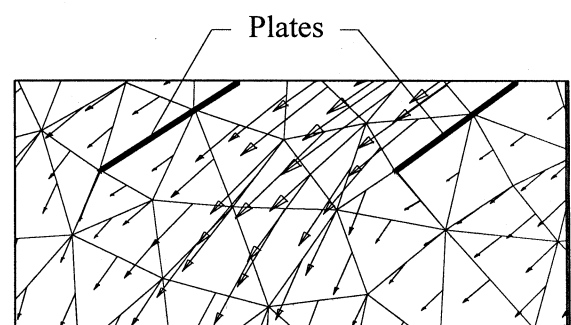


Fig. 14 - Detail of flow behavior in the area highlighted in Fig. 13.

evaluated by several example problems that have exact solutions and/or experimental data before applying to solve more complex flow problems. Two selected examples that have exact solutions and an application of complex flow behavior through an uncommon shape of duct with varying cross-sectional area are presented in this paper. These example problems demonstrate the capability of the finite element formulations and the computer programs that can provide insight to the complex flow behaviors in order to help correcting problems as well as improving the design.

## 5. Acknowledgment

The author is pleased to acknowledge the Thailand Research Fund (TRF) and the National Research Council of Thailand (NRCT), Bangkok, Thailand, for supporting this research work.

## 6. References

1. Cook, R. D., Malkus, D. S. and Plesha, M. E., Concepts and Applications of Finite Element Analysis, Third Ed., Wiley & Sons, New York, 1989.
2. Zienkiewicz, O. C. and Taylor, R. L., The Finite Element Method, Fourth Ed., McGraw-Hill International, 1991.
3. Lewis, R. W., Morgan, K., Thomas, H. R., and Seetharamu, K. N., The Finite Element Method in Heat Transfer Analysis, John Wiley & Sons, New York, 1996.
4. Dechaumphai, P., Finite Element Method in Engineering, Chulalongkorn University Press, Bangkok, 1994.
5. Jin, J., The Finite Element Method in Electromagnetics, John Wiley & Sons, New York, 1993.
6. Gallagher, R. H., Simon, B. R., Johnson, P. C. and Gross, J. F., Finite Elements in Biomechanics, John Wiley & Sons, New York, 1982.
7. Peraire, J., Vahidati, M., Morgan, K., and Zienkiewicz, O. C., "Adaptive Remeshing for Compressible Flow Computation," *J. of Comp. Phys.*, Vol. 72, 1987, pp. 449-446.
8. Dechaumphai, P., "Adaptive Finite Element Technique for Heat Transfer Problems," *J. of Energy, Heat & Mass Transfer*, Vol. 17, No. 2, 1995, pp. 87-94.
9. Yamada, Y., Ito, K., Yokouchi, Y., Yamano, T. and Ohtsubo, T., "Finite Element Analysis of Steady Fluid and Metal Flow," *Finite Element in Fluid*, Edited by Gallagher, R. H., et. al., John Wiley and Sons, New York, 1975.
10. White, F. M., Viscous Fluid Flow, Second Ed., McGraw-Hill, New York, 1991.
11. Dechaumphai, P., Numerical Methods in Engineering, Chulalongkorn University Press, Bangkok, 1995.